AIAA 2001-4006

The Impact of Structural Vibration on Flying Qualities of a Supersonic Transport

David L. Raney, E. Bruce Jackson,
Carey S. Buttrill, and William M. Adams
NASA Langley Research Center
Hampton, VA 23681-2199

AIAA Atmospheric Flight Mechanics Conference
6-9 August 2001
Montreal, Canada

The Impact of Structural Vibration on Flying Qualities of a Supersonic Transport

David L. Raney*, E. Bruce Jackson§, Carey S. Buttrill†, and William M. Adams‡
NASA Langley Research Center
Hampton, VA 23681-2199

ABSTRACT

A piloted simulation experiment has been conducted in the NASA Langley Visual/Motion Simulator facility to address the impact of dynamic aeroelastic effects on flying qualities of a supersonic transport. The intent of this experiment was to determine the effectiveness of several measures that may be taken to reduce the impact of aircraft flexibility on piloting tasks. Potential solutions that were examined included structural stiffening, active vibration suppression, and elimination of visual cues associated with the elastic modes. A series of parametric configurations was evaluated by six test pilots for several types of maneuver tasks.

During the investigation, several incidents were encountered in which cockpit vibrations due to elastic modes fed back into the control stick through involuntary motions of the pilot's upper body and arm. The phenomenon, referred to as *biodynamic coupling*, is evidenced by a resonant peak in the power spectrum of the pilot's stick inputs at a structural mode frequency.

The results of the investigation indicate that structural stiffening and compensation of the visual display were of little benefit in alleviating the impact of elastic dynamics on the piloting tasks, while increased damping and elimination of control-effector excitation of the lowest frequency modes offered great improvements when applied in sufficient degree.

INTRODUCTION

As commercial transport aircraft designs become larger and more flexible, the impact of aeroelastic vibration on the vehicle's flight dynamics, flight control, and flying qualities increases in prominence. The consideration of such effects assumed unprecedented significance in the design of the Boeing High Speed Civil Transport (HSCT). Constraints imposed by flight at supersonic speeds resulted in a very large but relatively light and slender vehicle design that exhibited unusually low-frequency aeroelastic modes. The resulting low frequency cockpit vibrations had significant potential to negatively influence the pilot's ability to maneuver the aircraft, not only due to the degradation of ride quality but also due to adverse coupling between the human pilot's control dynamics and the configuration's aeroelastic dynamics.

A piloted simulation experiment was therefore conducted in the Langley Visual/Motion Simulator (VMS) facility to address the impact of dynamic aeroelastic effects on flying qualities of the High-Speed Civil Transport. The primary objective of this investigation was to determine the effectiveness of measures that may be taken to reduce the impact of aircraft flexibility on piloting tasks for the HSCT. The secondary objective was to establish preliminary guidelines for designing a structural mode control system for an HSCT concept.

An earlier motion-based simulation study using a dynamic aeroelastic HSCT model in the Langley VMS facility revealed a significant reduction in the ease with which piloted approach and landing tasks were performed when dynamic elastic modes were included in the model.[1] An even earlier investigation by Schmidt and Waszak had also been conducted in the Langley VMS, illustrating the potentially detrimental effects of dynamic elasticity on the flying qualities of a flexible B1 aircraft simulation in 1985.[2] The potential for such effects had been noted in a 1983 report by Ashkenas, Magdaleno and McRuer that cautioned of implications of structural flexibility for the flying qualities of large aircraft.[3]

---

* Research scientist, Dynamics and Control Branch, MS 406, Senior Member AIAA.
§ Research scientist, Dynamics and Control Branch, MS 149, Senior Member AIAA.
† Research scientist, Systems Development Branch, MS 125B, Senior Member AIAA.
‡ Distinguished Research Associate, Dynamics and Control Branch, MS 406, Senior Member AIAA.

The approach of the present investigation was to vary certain parameters in the aeroelastic model to provide a simplified representation of several potential means of alleviating the impact of dynamic aeroelasticity on piloting tasks. The potential solutions that were examined consisted of 1) increasing the frequency of the elastic modes, 2) increasing the damping of various combinations of elastic modes, 3) elimination of control effector excitation of the lowest frequency elastic modes, and 4) elimination of visual cues associated with the elastic modes.

Approximate representations for each of these potential solutions were generated in the simulation model by directly parameterizing the modal frequencies and damping, as well as control input and visual output effects. By exploring parametric variations in each of these factors, information was gained regarding the effectiveness of each approach, and the degree to which it must be exercised in order to achieve the desired flying qualities improvement. A total of 20 parametric configurations were evaluated by six test pilots representing the FAA (1), Boeing (1), NASA (2), and Calspan (2).

HSCT SIMULATION MODEL

This experiment used a mathematical simulation of the so-called "Cycle 3" version of the "Reference-H" supersonic transport design. [1] The model was published by Boeing Commercial Aircraft Group in the summer of 1996 as the fourth major release in a series of increasingly detailed math models of the Reference-H configuration. The simulation model was based upon a combination of wind tunnel and computational fluid dynamics studies of the Reference-H design, ranging from low subsonic to Mach 2.4 supersonic wind tunnel studies.

Finite-element structural models were used to predict the effect of steady flight loads upon aerodynamic stability derivatives, referred to as quasi-static aeroelastic effects (QSAE). A key feature of the math model was the inclusion of dynamic aeroservoelastic effects (DASE), which required additional states to represent the flexible modes of the aircraft structure.

General Configuration Description

The Reference-H vehicle design has a cranked-arrow planform with a conventional aft tail and four under-wing engines. The control devices include an independently actuated horizontal stabilizer and elevator, a three-segment rudder on a fixed vertical fin, eight trailing-edge flaperons (four per wing), and leading-edge flaps.

The vehicle is designed to carry 300 passengers a distance of approximately 5,000 nautical miles. The aircraft has an operating empty weight of 280,000 lb and a maximum takeoff gross weight of 650,000 lb. Final cruise weight is expected to be 385,000 lb.

The length of the HSCT configuration is approximately 310 ft, with a wingspan of 130 ft. The HSCT's length and slenderness result in very low-frequency structural modes, with the first symmetric bending mode occurring at approximately 1.25 Hz. As a point of reference, the length of the Concorde is approximately 204 ft, the length of the Tu-144 is 215 ft, and the B1 is approximately 135 ft. The HSCT planform is shown in Figure 1, super-imposed with a planform of the B1 configuration for scale comparison.

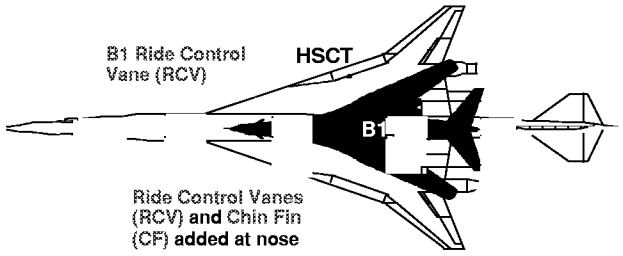

Figure 1. Comparison of HSCT and B-1 planforms.

The B1 uses an active vibration suppression control system to improve ride quality at the cockpit station. Small active control surfaces called ride control vanes are located near the pilot station of the B1 to damp vertical vibrations at the cockpit. The Boeing HSCT design is equipped with similar devices for active suppression of vertical vibrations as noted in Figure 1. Additionally, a vertical "chin fin" is included in the HSCT design for active suppression of lateral cockpit vibrations.

Dynamic Aeroelastic Effects

The dynamic aeroelastic portion of the model used in this simulation experiment contained six flexible aircraft modes, 3 symmetric and 3 antisymmetric. The mode shapes and their associated in-vacuo frequencies are shown in Figure 2. The model was generated for a flight condition of Mach 0.24 at a weight of 384,862 lb and a cg location at 53.2% of the mean aerodynamic chord, which constitutes the landing condition.

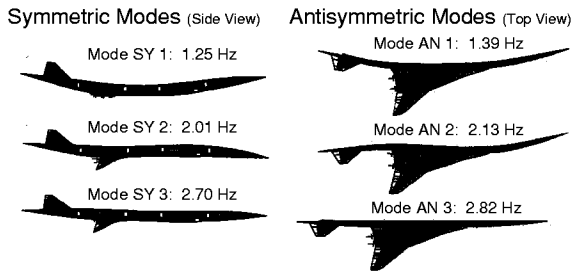

Figure 2. Aeroelastic mode shapes and in-vacuo frequencies used in simulation.

Dynamic aeroelastic modes contained in the model could be excited by turbulence and by control effector movements. No inputs from landing gear reaction forces or engine pylon reaction forces were included in the model.

Visual effects of the structural flexibility were provided in the simulation. The out-the-window scene that was presented on the cockpit monitors moved in relation to the Head-Up Display (HUD) to represent local perturbations in pitch and yaw at the pilot station. The overall effect was that the out-the window scene appeared to bounce slightly both vertically and laterally in response to elastic excitation. These visual perturbations were typically on the order of $\pm$ 0.1 degrees during maneuvers performed with dynamic aeroelastic effects.

Parameterized Aeroelastic Characteristics

The baseline aeroelastic model described above was parameterized to provide the ability to systematically vary several characteristics of the piloted simulation. These modifications allowed the impact of structural stiffening, modal damping, modal cancellation and visual cues to be evaluated from a piloted control standpoint.

Variation of Structural Stiffness

The variation of structural stiffness was represented by multiplying the frequencies of all six elastic modes by a given frequency ratio. The representation of structural stiffening by directly manipulating the model in this fashion is clearly approximate, but appeared sufficient to capture the basic effect. Frequency ratios of 1.0 (baseline), 1.16 ("stif1" configuration), 1.36 ("stif2") and 1.60 ("stif3") were chosen. This selection produced first symmetric bending mode frequencies of 1.25 Hz, 1.45 Hz, 1.80 Hz and 2.0 Hz. Aeroelastic simulation models were produced for each of these conditions.

Figure 3 illustrates the migration of the dynamic elastic poles that occurred as the stiffness level was varied. The total range of variation probably extends beyond the conditions that would be physically practical for this design because of the weight penalties associated with producing the stiffer structure. Aircraft weight was not increased in the simulation as the modal frequencies were increased.

The "stif1" condition of 1.45 Hz for the first symmetric mode was considered to be most representative of the actual configuration, and so was used as the modified baseline configuration for all other parametric variations. Acceleration time histories from the motion-based simulation were used to verify that this parameterization method produced the desired effect.

Configuration	Frequency Ratio	Stiffness Increase	1st SY Mode Frequency
baseline	1.00	--	1.25 Hz
stif1	1.16	~35%	1.45 Hz
stif2	1.36	~85%	1.80 Hz
stif3	1.60	~150%	2.00 Hz

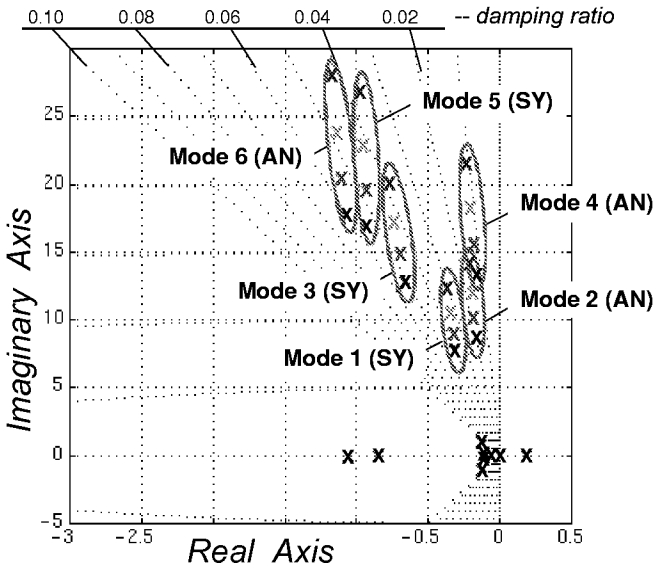

Figure 3. Migration of elastic mode poles with structural stiffness variation.

Variation of Modal Damping

The portion of the test matrix that varied the modal damping level actually targeted several issues. The first issue was the effect of the amount of damping that was applied to the dynamic elastic modes. Damping ratios of 0.07, 0.15, and 0.30 were selected based on feedback obtained during an HSR Dynamic Aeroelastic Model Working Group meeting that was held in August of 1997.

The second issue dealt with the frequency range of the modes to which damping was applied. In the first variation, damping was applied only to elastic modes with frequencies

less than 2 Hz. This range included the first symmetric mode at 1.45 Hz and the first antisymmetric mode at 1.62 Hz. In the second variation, damping was applied to elastic modes with frequencies less than 3 Hz. This range included the first two symmetric and the first two antisymmetric modes. The intent was to examine the effect of damping only the first fuselage bending modes as compared to the first and second fuselage harmonics shown in Figure 2.

Figure 4 illustrates the migration of the dynamic elastic poles that occurred as increased damping was applied in these two frequency ranges. The frequency response plots shown in Figure 5 illustrate the attenuation of the elastic response to control inputs that results from the increased damping levels applied to modes with frequencies less than 3 Hz. Vertical acceleration at the pilot station (Nz ps) in response to elevator inputs and lateral acceleration at the pilot station (Ny ps) in response to rudder inputs are shown.

An additional issue that was addressed by this portion of the test matrix was the relative importance of suppressing symmetric modes versus antisymmetric modes. In both frequency ranges, a damping ratio of 0.3 was applied to the symmetric modes alone (configurations "damp4" and "damp9") and then the antisymmetric modes alone (configurations "damp5" and "damp10").

Configuration	Damping Ratio	Modes
stif1	nominal	—
damp1	0.07	SY1, AN1
damp2	0.15	SY1, AN1
damp3	0.30	SY1, AN1
damp4	0.30	SY1
damp5	0.30	AN1
damp6	0.07	SY1-2, AN1-2
damp7	0.15	SY1-2, AN1-2
damp8	0.30	SY1-2, AN1-2
damp9	0.30	SY1-2
damp10	0.30	AN1-2

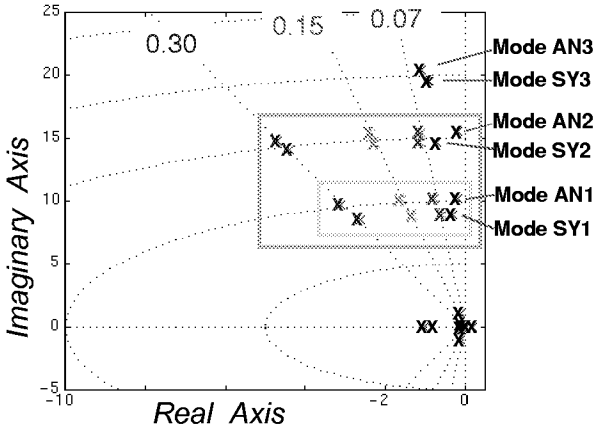

Figure 4. Migration of the dynamic elastic poles with damping level variation.

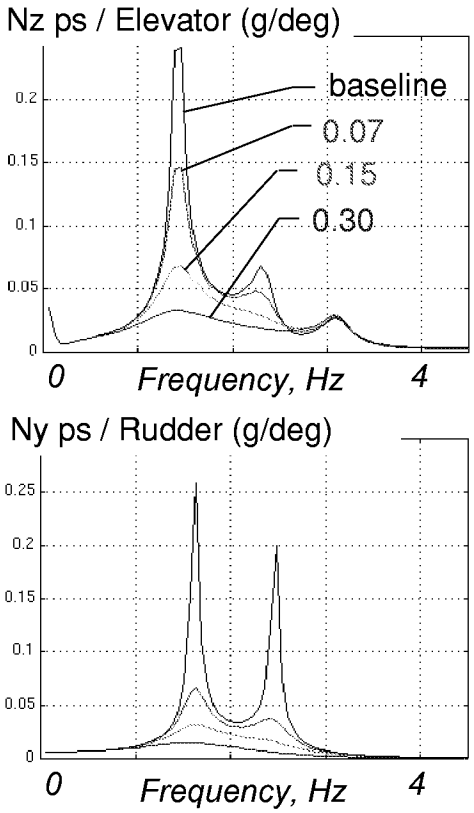

Figure 5. Variation of frequency response to control inputs for various damping levels.

A total of 10 parametric conditions were included in the damping portion of the test matrix. Again, since the model was directly manipulated to produce the desired damping levels, the representation of an active mode suppression system is approximate and lacks nonlinearities and additional filter dynamics that might be present in the actual system.

Impact of Modal Cancellation

Another portion of the test matrix examined the impact of *modal cancellation*. This term refers to the elimination of the control effector excitation of a particular elastic mode or modes. Such a modification allows the control system to pitch, roll, or yaw the aircraft without exciting the specifically targeted modes. It is intended to represent the effect that would be produced by using multiple control effectors in appropriate proportion (canard and elevator for instance) to pitch the vehicle without exciting the first fuselage bending mode. In the lateral case, it represents the use of rudder and chin fin in combination to avoid excitation of the first antisymmetric mode.

Configuration	Modes Canceled	Modes Damped
stif1	none	none
canc1	SY1, AN1	none
canc2	SY1, AN1	1-4 @ 0.07
canc3	SY1, AN1	1-4 @ 0.15
canc4	SY1, AN1	1-4 @ 0.30

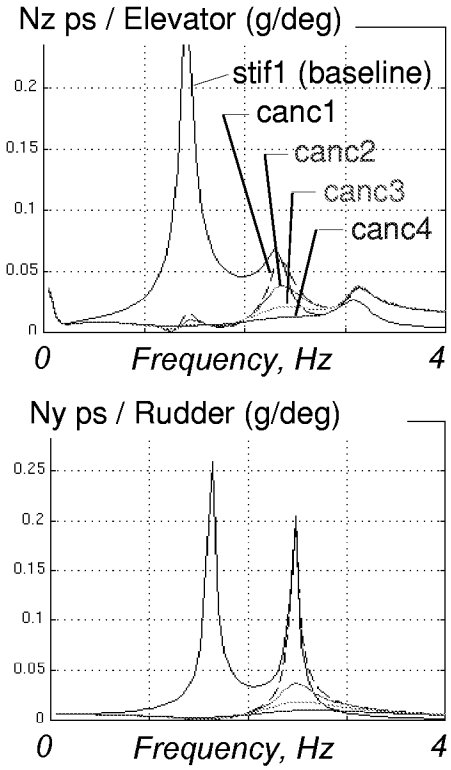

Figure 6. Variation in frequency response to control inputs for mode-canceled configurations.

The effect of such a mode-canceling control system was approximated by eliminating the elements of the B matrix in the dynamic aeroelastic model that represent the control effector excitation inputs to the first symmetric and first antisymmetric fuselage bending modes. Mode-canceling configurations were generated for each of the three damping levels so that the test matrix would include direct comparisons of cancellation on and off for each of these damping conditions.

Figure 6 illustrates the change in frequency responses that resulted from this modification. The plots show that the first symmetric and first antisymmetric modes can no longer be excited by control inputs for the canceled configurations. The modal dynamics remain, however, and are subject to excitation by turbulence or by coupling from other elastic modes. Cancellation was applied only to the first symmetric and first antisymmetric modes, since cancellation of higher fuselage harmonics would probably require more control effectors. This representation is inherently approximate since it cannot depict the effect of nonlinearities that would be present in an actual mode suppression system such as control saturation or rate limiting.

THE LANGLEY VISUAL/MOTION SIMULATOR

The Langley Visual Motion Simulator (VMS), shown in Figure 7, uses a synergistic hexapod motion system. The motion platform provides up to ±0.6 g acceleration cues vertically within a 5.75 foot travel envelope; lateral and longitudinal acceleration limits are similar.[4] The angular limits of the platform are +30/–20° pitch, ±32° yaw, and ±22° roll. (Positive pitch is in the nose up direction.)

Linear Accelerations, g

Surge: ± 0.6 Sway: ± 0.6 Heave: ± 0.8

Angular Accelerations, deg/s ^{2}

Roll: ± 50 Pitch: ± 50 Yaw: ± 50

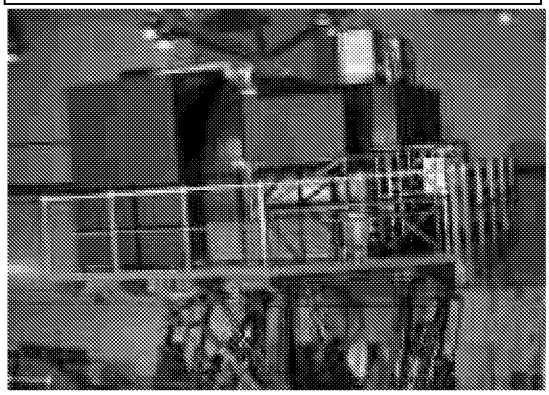

Figure 7. Langley Visual/Motion Simulator (VMS) and its acceleration capabilities.

The cockpit configuration at the time of this experiment included a left seat pilot's station and a right seat observer's station. A four-lever throttle quadrant was located between the two stations. A McFadden left-handed side stick controller was used for all maneuvers performed during this experiment. The pilot station included an armrest that was adjustable to provide appropriate forearm support for the left arm of the evaluation pilot.

Refinements were made to the motion drive algorithms to improve the suitability of the simulator for representing the aeroelastic motion cues. The motion commands produced by the dynamic elastic portion of the aircraft model generally bypassed the motion washout filters to avoid any attenuation or delay of the elastic vibration cues.

Figure 8 was taken from a 1973 report which documented the frequency response capabilities of the Langley VMS Motion facility.[4] The input/output amplitude ratios for vertical (z) and lateral (y) sinusoidal inputs of 1.8 inches are shown, along with the resulting phase lag, for input frequencies from 0.1 to 12 rad/sec. Also shown on these plots is the frequency range of the dynamic elastic modes that were included in the earlier (LaRC.1) assessment.[1]

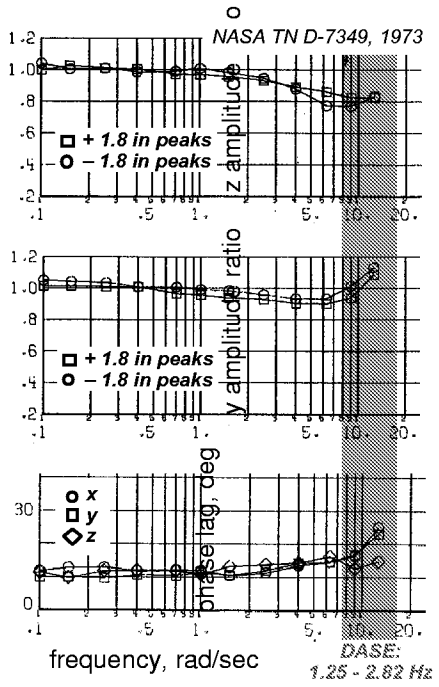

Figure 8. Frequency response of Langley Visual/Motion Simulator as documented in NASA TN D-7349, 1973.

The dynamic elastic portions of the model caused the motion platform to operate at the threshold of its capabilities. The simulator provides reasonable performance (0.8 amplitude ratio vertically and 1.0 amplitude ratio laterally, with about 15 deg of phase loss) at the lowest structural mode frequencies (1.25 and 1.39 Hz). The next two dynamic elastic modes (at 2.0 and 2.1 Hz) lie marginally within the motion platform's capabilities with about 25 deg of phase loss. Based on cockpit accelerometer time histories, the facility appeared to provide a reasonable representation of the modes that were included in the dynamic aeroelastic model.

EVALUATION SCALES

The familiar Cooper-Harper rating (CHR) scale was used during pilot evaluations of the parametric aeroelastic configurations. After completing a sufficient number of runs to rate a particular configuration, the test pilot's evaluations and comments were recorded. The pilot's task performance, in terms of touchdown parameters or flight-director tracking accuracy, was provided on a cockpit display immediately following each run. This information provided an indication of whether desired or adequate performance tolerances had been achieved, thus helping the pilot to navigate through the Cooper-Harper decision tree.

In addition to Cooper-Harper Ratings, the pilots were asked to provide an assessment of the extent to which dynamic elastic effects adversely impacted their control inputs and ride quality. The rating scales for these assessments are shown in Figure 9 and Figure 10.

DASE INFLUENCE ON RIDE QUALITY	RQR
Cockpit vibrations do not impact ride quality.	1
Cockpit vibrations are perceptible but not objectionable - no improvement necessary.	2
Cockpit vibrations are mildly objectionable - improvement desired.	3
Cockpit vibrations are moderately objectionable - improvement warranted.	4
Cockpit vibrations are highly objectionable - improvement required.	5
Cockpit vibrations cause abandonment of task - improvement required.	6

Figure 9. Evaluation scale for dynamic aeroelastic influence on ride quality.

DASE INFLUENCE ON PILOT'S CONTROL INPUTS	CIR
Pilot does not alter control inputs as a result of aircraft flexibility.	1
Pilot intentionally modifies control inputs to avoid excitation of flexible modes.	2
Cockpit vibrations impact precision of voluntary control inputs.	3
Cockpit vibrations cause occasional involuntary control inputs.	4
Cockpit vibrations cause frequent involuntary control inputs.	5
Cockpit vibrations cause sustained involuntary control inputs or loss of control.	6

Figure 10. Evaluation scale for dynamic aeroelastic influence on pilot's control inputs.

These supplemental rating scales were designed for this experiment and are intended to target the acceptability of a particular aeroelastic

configuration apart from deficiencies that the pilot may perceive in the nominal flight control system. For instance, if a pilot awards the landing task a CHR of 4, but provides a DASE Control Influence Rating (CIR) of 1 and a DASE Ride Quality Rating (RQR) of 1, then we might conclude that the deficient CHR is due to pilot dissatisfaction with the baseline flight control system, and not with the dynamic aeroelastic characteristics of that particular configuration.

The CIR Scale shown in Figure 10 bears further discussion. The scale was developed based on pilot comments from the earlier (LaRC.1) piloted assessment of dynamic aeroelastic effects. Pilots sometimes indicated that they were "reducing the gain" or "backing off" on their control inputs to avoid excitation of the elastic modes. Several time histories from the LaRC.1 test suggested that the cockpit vibration environment had sometimes corrupted the precision of pilot control inputs, or even caused occasional involuntary stick inputs that have been referred to as *biodynamic feedthru*.[3] The Control Influence Rating Scale was developed to specifically address this issue apart from the pilot comfort or ride quality issue. Pilot feedback was incorporated during the design of the CIR and RQR scales prior to this experiment.

EVALUATION MANEUVERS

The tasks that were evaluated during this investigation included an up-and-away flight director tracking task, a nominal approach and landing, and a lateral-offset landing task. The offset landing was the most challenging of the three evaluation maneuvers. This task was initiated at an altitude of 750 ft with a 300-ft lateral offset and 580 ft longitudinal offset of the instrument landing system (ILS) approach glide-slope from the nominal approach path. The pilot was directed to fly down the offset glideslope to an altitude of 250 ft. At this point, the test conductor called "Correct," and the pilot executed a lateral correction and vertical descent to re-acquire the runway centerline. The pilot then executed a flare and attempted to achieve touchdown within the tolerances required for desired performance. The task required an aggressive lateral maneuver due to the low altitude at which the correction was initiated. The lateral offset landing is a standard evaluation maneuver used in Calspan's Total In-Flight Simulator (TIFS) aircraft flight tests.

The intent of the flight director tracking task was to cause the pilot to exercise a wide range of control input frequencies. The flight director presented on the pilot's HUD was driven with a signal containing segments from various maneuvers that had been examined in previous HSCT simulations. These segments included a localizer capture, a glideslope capture, a descending turn, and a rapid pull-up as performed during an aborted landing task. Flight path and track angle command segments from these tasks were combined with varying order and sign to produce a flight director behavior that was not easily anticipated, but was still representative of actual flight maneuver tasks.

Each of the parametric aeroelastic configurations were evaluated using each of the 3 maneuver tasks described above. All tasks were performed in the presence of mild turbulence that was produced using a Dryden spectra turbulence model.

RESULTS AND DISCUSSION

Configuration Preference Ranking

Figure 11 presents a ranking of the 20 parametric aeroelastic configurations based on the average of the DASE Control Influence Ratings and Ride Quality Ratings that were assigned by all the pilots for all three maneuver tasks performed with a given configuration. Cooper-Harper Ratings did not seem to discriminate among configurations as clearly as the CIR and RQR ratings which specifically targeted DASE effects, and their impact has not been included in this ranking.

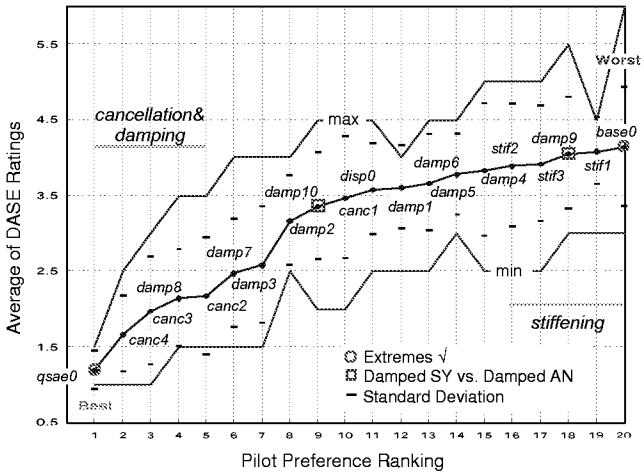

Figure 11. Pilot preference ranking of configurations based on DASE ratings.

The ranking exhibits a number of trends that would appear to make intuitive sense. First, the baseline aeroelastic configuration (base0), with no structural stiffening or active mode

suppression, was ranked as the worst configuration. Also reassuringly, the rigid (quasi-static effects only) configuration without any dynamic aeroelastic effects (qsae0) was ranked the best.

Differentiation among configurations is greatest at the start of the ranking, in the most desirable region, and tapers off to near-ties at the undesirable end of the spectrum. The stiffened cases without active mode suppression were all ranked poorly, suggesting that this approach was not effective at reducing the impact of cockpit vibration on piloting tasks. The configuration with the greatest number of modes damped (4) at the greatest level (0.3) and with modal cancellation (canc4) was rated the best of the flexible configurations, but was still very noticeably different from the rigid aircraft (qsae0). The next-best case was identical to this one with the exception of damping level, which was reduced to 0.15 (canc3). The fourth ranked configuration had 0.3 damping on 4 modes, but had no cancellation (damp8).

The order of ranking provides some interesting insights regarding potential trades between mode-canceling control and additional damping. Another insight is gained when we compare the rankings of the configuration which had only symmetric modes damped (damp9, ranked 18th) with the configuration which had only antisymmetric modes damped (damp10, ranked 9th). It is clear that the pilots found the undamped antisymmetric motions to be more problematic than undamped symmetric motions.

A comparison of the disp0 configuration with the damp1 configuration indicates that the elimination of vibration-induced perturbations in the visual scene provided little or no benefit according to this ranking. These configurations were identical in all respects other than the lack of vibration-induced perturbations in the out-the-window scene for the disp0 configuration.

Ride Quality Ratings vs. Pilot Preference

The ranking in the previous figure provides insight regarding the order of pilot preference for the 20 parametric configurations, but does not indicate the point in the ranking at which dynamic elastic characteristics make the configuration unacceptable. Figure 12 shows the average Ride Quality Rating assigned by the pilots for each configuration plotted against the Pilot Preference Ranking from the previous figure. The RQR assigned by the pilots is shown adjacent to the ride quality axis, along with shading to indicate the transition from acceptable to marginal to unacceptable configuration characteristics. On the basis of the average ratings, the first four configurations (qsae0, canc4, canc3, and damp8) appear to be in or on the border of the acceptable ride quality region.

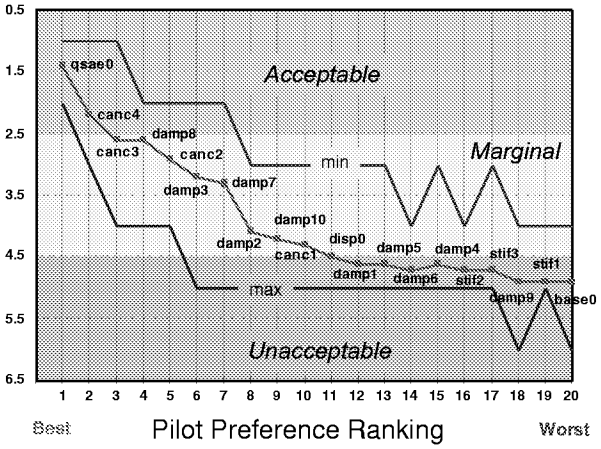

Figure 12. Average ride quality rating vs. preference ranking of parametric configurations.

Also shown on the plot are the maximum and minimum ride quality ratings assigned to the configurations. On the basis of the maximum rating, even the most highly mode-suppressed configuration (canc4) provides only marginally acceptable ride quality at the pilot station. It should be noted that these ratings were provided during tasks that were performed with mild turbulence, and that the ride quality acceptability will probably vary with turbulence level. This plot provides a subjective basis for the judgment of an acceptable level of mode suppression from the pilot's ride-quality perspective.

Control Influence Ratings vs. Pilot Preference

This chart provides an analogous ranking to the previous chart in terms of the Control Influence Rating instead of Ride Quality Rating. The CIR assigned by the pilots is shown adjacent to the control influence axis, along with shading to indicate the transition from acceptable to marginal to unacceptable configuration characteristics. Based on discussions with the test pilots prior to the experiment, it was decided that the unacceptable threshold should be placed at the point at which cockpit vibrations impact the precision of voluntary control inputs.

On the basis of the average control influence ratings, the first four configurations (qsae0, canc4, canc3, damp8) again lie within the acceptable region. Each of the acceptable elastic configurations applies a damping level of 0.3 to the first two symmetric and first two antisymmetric modes. On the basis of the

maximum rating, the most highly mode-suppressed configuration (canc4) again lies in the marginal control influence region.

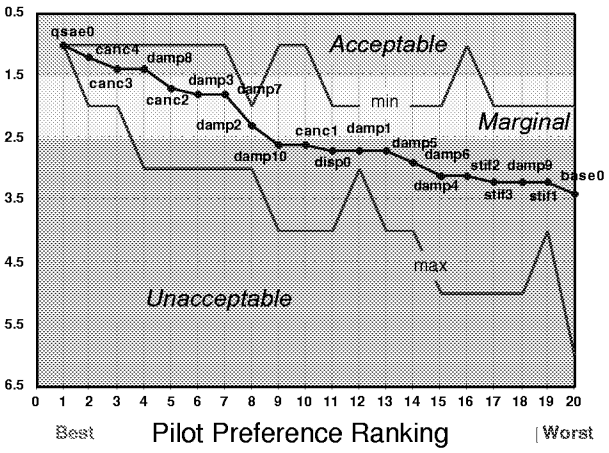

Figure 13. Average control influence rating vs. preference ranking for parametric configurations

The border between acceptable and marginal control influence on this plot is somewhat arbitrary, since it might be perfectly acceptable for the pilots to intentionally modify their control inputs to avoid excitation of the dynamic elastic modes as long as their ability to precisely control the aircraft is in no way hindered by this practice. However, recorded time histories of pilot stick deflections indicate that pilots were sometimes unaware that cockpit vibrations were in fact impacting their control inputs.

The occurrence of biodynamic feedthru of cockpit vibrations through the pilot's arm and back into the control stick is involuntary and therefore may indeed be unnoticed by the pilot in minor instances. Use of the Control Influence Rating scale shown in the figure requires the pilot to be aware of the occurrence, and therefore the CIR ratings may sometimes be optimistic. There were, however, a number of profound instances of frequent or sustained biodynamic feedthru of cockpit vibrations into the control stick as indicated by the maximum CIR ratings shown on the figure. Frequent or sustained feedthru of cockpit vibrations through the pilot's arm and back into the stick will be referred to as *Biodynamic Coupling* (BDC) in this report.

Example of Biodynamic Coupling Incident

Figure 14 presents a power-spectrum analysis of a lateral offset landing run in which the pilot experienced biodynamic coupling while flying the stif1 configuration with no additional damping or cancellation. The time history at the top of the figure shows lateral cockpit accelerations in g's (dashed line) and lateral stick deflections (solid line). Although the units on the two quantities differ, the scaling of ± 1 is convenient since it represents the maximum throw for lateral stick deflection and since lateral g's commanded by the simulation remained in the range of $\pm$ 1 g. The plot in the lower left of the figure shows the power spectral density of lateral accelerations and lateral stick deflections applied to a 6-second segment of the time history (from 37 to 43 seconds).

The frequency spectrum of the pilot's voluntary control inputs during this period lies primarily below 1 Hz. The frequency spectrum of the lateral accelerations at the pilot station shows some content at the first antisymmetric mode frequency of 1.6 Hz and the second antisymmetric mode frequency of 2.5 Hz due to minor turbulence excitation of these structural modes. (Recall that the frequencies shown in Figure 2 were multiplied by a factor of 1.16 to produce the "stif1" modified baseline.)

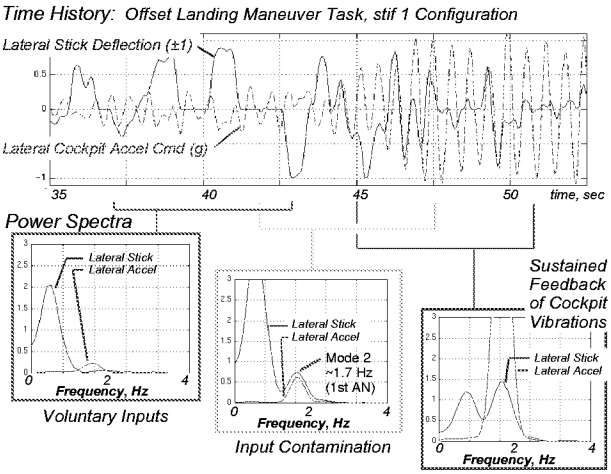

Figure 14. Power-spectrum analysis of biodynamic coupling incident for pilot B.

The power spectrum of a later 6-second segment of the time history (from 41 to 47 seconds) indicates the bulk of the pilot's input spectrum remains below 1 Hz, but it also shows some frequency content of the pilot's inputs in the range of the lateral elastic modes. Once the pilot begins to move the stick at the resonant frequency of the first antisymmetric structural mode there is tremendous potential for the lateral mode to be excited by the control inputs, producing larger lateral accelerations at the pilot station. These lateral accelerations can move the pilot's frame in a fashion which produces involuntary control inputs that further excite the structural mode.

The third power spectrum plot shown in Figure 14 is applied to a 6-second segment of the time history from 45 to 51 seconds. Here, the spectrum of the pilot's stick input exhibits a pronounced resonant peak at the frequency of the first antisymmetric structural mode. It is highly unlikely that the pilot's inputs in this frequency range are voluntary. Video footage of the cockpit interior along with footage of the pilot's hand on the sidestick depicts a strong correlation between the involuntary motions of the pilot's upper body with his control inputs. A clear change in the character of the pilot's stick inputs is apparent in the time history, as lateral accelerations feed through the pilot's frame and back into the control stick. The pilot would break the involuntary coupling loop if he released the stick, but he is in the midst of the flare and therefore unwilling to do so. In this instance the run was terminated by the co-pilot who hit the simulator "kill switch" due to the abusive ride quality.

This type of adverse biodynamic interaction between pilot and aircraft dynamics is not entirely unprecedented. An investigation performed at Dryden Flight Research Center identified a similar phenomenon involving the use of a sidestick control input in the F-16XL which resulted in roll ratcheting during abrupt high-rate rolling maneuvers.[5] The researchers produced an analytical model of the coupled system including dynamics of the pilot's frame and the control stick. The dynamics involved appeared somewhat similar to those encountered during the incidents of lateral biodynamic coupling in the present experiment. Dryden researchers identified a lateral resonant frequency of approximately 2.1 Hz for their combined pilot/control stick dynamic system.

Biodynamic Coupling Incidents for 3 Pilots

A number of incidents of biodynamic coupling were encountered when test pilots flew the HSCT with no active suppression of the lateral structural modes. At least three of the six test pilots encountered biodynamic coupling during some portion of the experiment. Pilots appeared most likely to couple with the configurations that had a 1st antisymmetric mode frequency in the range of 1.4 Hz to 2.2 Hz. Examples for pilots B, E, and C are shown in Figure 15. Power spectra of the pilots' stick inputs for each of these cases indicate a resonant peak at the frequency of the first antisymmetric elastic mode (mode AN1 in Figure 2).

Encounters with BDC were often catastrophic in terms their impact on the pilot's control of the aircraft. Note that Pilot C experienced coupling with the stif3 configuration, which has its first antisymmetric mode at a higher frequency than the stif1 baseline (2.2 Hz instead of 1.6 Hz.) The time histories shown for pilots B and E are for the damp 9 configuration, which actually applies 0.3 damping to the symmetric modes but leaves the antisymmetric modes undamped. The presence of significant damping for symmetric modes did little to prevent the coupling since the lateral axis is far more prone to BDC for a number of reasons.

First, the pilot's seat tends to support the body longitudinally and vertically, but not laterally, so side-to-side accelerations are more difficult to resist. Furthermore, symmetric modes produce vertical accelerations while the stick input is fore and aft, so there is less tendency for the pilot's body motions to feed directly into the stick. However, antisymmetric modes produce lateral accelerations which feed directly into lateral stick deflections. A sidestick control input device was used in this experiment. The susceptibility of various control input devices to biodynamic feedthru is a potential topic for future investigations and is a factor that clearly should be taken into consideration during design of the cockpit controls.

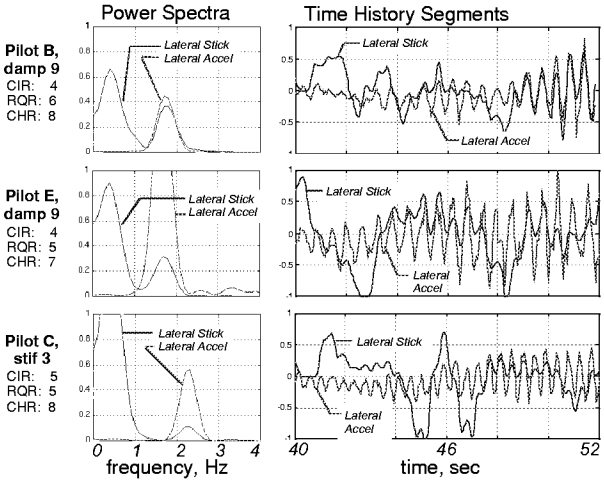

Figure 15. Examples of biodynamic coupling incidents for pilots B, E, and C.

One element of the control system that is implicated in the occurrence of BDC is the aileron-rudder interconnect (ARI). This is the control path whereby lateral stick displacements produce rudder deflections in proportion to aileron deflections to achieve turn coordination. But it is also the path whereby lateral cockpit vibrations may feed directly through the pilot/stick dynamics and back into rudder deflections, further exciting lateral elastic modes. It is

possible that some provision may be included in the design of the ARI to interrupt or prevent biodynamic coupling.

Structural stiffening did not provide relief from biodynamic coupling for the pilots who appeared most prone to this type of interaction. Damping levels of 0.15 applied to the first symmetric and first antisymmetric modes appeared sufficient to prevent biodynamic coupling for all pilots involved in the experiment.

The potential hazard posed by biodynamic coupling would seem to suggest that certain elements of an HSCT active mode suppression control system should be designated as flight critical. However, a final judgment regarding this issue should be made on the basis of evaluations performed with a higher fidelity dynamic aeroelastic model of the final aircraft configuration.

CONCLUDING REMARKS

A piloted simulation experiment has been conducted in the Langley Visual/Motion Simulator facility to address the impact of dynamic aeroelastic effects on flying qualities of a High-Speed Civil Transport. The intent of the experiment was to generate information regarding measures that may be taken to reduce the impact of aircraft flexibility on piloting tasks. Potential solutions that were examined consisted of increasing the frequency of the elastic modes, increasing the damping of various combinations of elastic modes, elimination of control effector excitation of the lowest frequency elastic modes, and elimination of visual cues associated with the elastic modes. A total of 20 parametric aeroelastic configurations were each evaluated by six test pilots.

During the investigation, several profound incidents of biodynamic coupling were encountered in which cockpit vibrations due to elastic modes fed back into the control stick through involuntary motions of the pilot's upper body and arm. The phenomenon is evidenced by a resonant peak in the power spectrum of the pilot's stick inputs at the frequency of one of the dynamic elastic modes. The tendency to couple with structural modes in this fashion appears to increase when pilots tighten their grip on the stick, often in preparation for the flare as the aircraft nears the runway.

Three of the six evaluation pilots encountered biodynamic coupling during the experiment. All of the pilots indicated that vibrations had impacted the precision of their inputs at some point in the experiment. Pilots were far more prone to experience adverse coupling with antisymmetric modes rather than symmetric modes. The severity of the biodynamic coupling phenomenon may have implications for control stick design and for the flight criticality of an active mode suppression control system.

The results of the investigation indicate that structural stiffening and compensation of the visual display were of little benefit in alleviating the impact of elastic dynamics on the piloting tasks, while increased damping and elimination of control effector excitation of the lowest frequency modes both offered great improvements when applied in sufficient degree.

Damping levels of 0.15 applied to the first symmetric and first antisymmetric modes appeared sufficient to prevent biodynamic coupling for all pilots who participated in the experiment. When damping levels of 0.3 were applied to the first two symmetric and first two antisymmetric modes, average pilot ratings indicated that an acceptable configuration was achieved.

REFERENCES

[1] Jackson, E. Bruce; Raney, David L; Hahne, David; Derry, Stephen D., NASA Langley Research Center, and Glaab, Louis J., Lockheed-Martin Engineering Services Company: "(LaRC.1) Pilot Briefing Guide", NASA TM, November 1996.

[2] Waszak, Martin R.; Schmidt, David K.: "Analysis of Flexible Aircraft Longitudinal Dynamics and Handling Qualities, Volumes I and II." NASA Contractor Report 177943, Grant NAG1-254, June 1985.

[3] Ashkenas, I.L.; Magdaleno, R.E.; McRuer, D.T.: "Flight Control and Analysis Methods for Studying Flying and Ride Qualities of Flexible Transport Aircraft". Systems Technology, Inc.; Contract NAS1-1847, NASA Contractor Report 172201, August 1983.

[4] Parrish, Russell V.; Dieudonne, James E.; Martin, Dennis J.; Copeland, James L.: "Compensation Based on Linearized Analysis for a Six-Degree-of-Freedom Motion Simulator", NASA TN D-7349, 1973.

[5] Smith, John W.; Montgomery, Terry: "Biomechanically Induced and Controller-Coupled Oscillations Experienced on the F-16XL Aircraft During Rolling Maneuvers", NASA TM 4752, Dryden Flight Research Center, Edwards, CA, 1996.